

Thermal radiation from optically driven Kerr ($\chi^{(3)}$) photonic cavitiesChinmay Khandekar,¹ Zin Lin,² and Alejandro W. Rodriguez¹¹*Department of Electrical Engineering, Princeton University, Princeton, NJ 08540*²*School of Engineering and Applied Sciences, Harvard University, Cambridge, MA 02139*

We study thermal radiation from nonlinear ($\chi^{(3)}$) photonic cavities coupled to external channels and subject to incident monochromatic light. Our work extends related work on nonlinear mechanical oscillators [Phys. Rev. Lett. 97, 110602 (2006)] to the problem of thermal radiation, demonstrating that bistability can enhance thermal radiation by orders of magnitude and result in strong lineshape alternations, including “super-narrow spectral peaks” occurring at the onset of kinetic phase transitions. We show that when the cavities are designed so as to have perfect linear absorptivity (rate matching), such thermally activated transitions can be exploited to dramatically tune the output power and radiative properties of the cavity, leading to a kind of Kerr-mediated thermo-optic effect. Finally, we demonstrate that in certain parameter regimes, the output radiation exhibits Stokes and anti-Stokes side peaks whose relative magnitudes can be altered by tuning the internal temperature of the cavity relative to its surroundings, a consequence of strong correlations and interference between the emitted and reflected radiation.

Driven nonlinear oscillators, including optical,¹ optomechanical,² and MEMS^{3,4} resonators, have been studied for decades and exploited for many applications, from mass detection⁵ to sensing⁶ and tunable filtering.⁷ When driven to a non-equilibrium state, these systems can exhibit a wide range of unusual thermal phenomena,⁸ leading for instance to cooling and amplification of thermal fluctuations in optomechanical systems,² generation of squeezed states of light in Kerr media,⁹ and stochastic resonances.¹⁰ Previous studies of Duffing oscillators have also identified novel effects arising from the nonlinear interaction of coherent pumps with thermal noise,^{11–13} leading to phase transitions and lineshape alterations that were recently observed in a handful of systems, e.g. mechanical oscillators^{14,15} and Josephson junctions.¹⁶

In this letter, we study thermal radiation effects in optically driven $\chi^{(3)}$ photonic cavities coupled to external channels. We demonstrate that in certain parameter regimes, bistability^{17,18} in photonic resonators leads to thermally activated transitions that amplify thermal fluctuations by orders of magnitude and cause dramatic changes in the cavity spectrum, analogous to noise-induced switching in mechanical oscillators.¹⁵ We find that when the photonic cavity is critically coupled to the radiation channel (enforced by designing the cavity to have equal dissipation and radiation rates),¹⁹ the coherent part of the output power varies dramatically with temperature, leading to a kind of Kerr-mediated thermo-optic effect. A simple perturbative analysis also shows that outside of the bistability region, the interaction of the coherent drive with thermal noise leads to amplified, Raman-type Stokes and anti-Stokes side peaks in the radiation spectrum, the relative amplitudes of which depend on a sensitive interference between the externally incident and reflected thermal radiation. Related phenomena have been long studied¹³ and more recently observed^{14,15} in the context of driven nonlinear mechanical oscillators as well as resonators based on rf-driven Josephson junctions¹⁶, and microscopic theories have also been used to describe related optical effects in the quantum regime.²⁰ Our work is an extension of these studies to the particular problem of thermal radiation from photonic resonators. As we show below, additional considerations arising in the case of radiation from cavities but absent in mechanical oscillators or bulk media, such as the strong coupling of the cavity to an external channel, dramatically impact the outgoing radiation. The ability to tune the radiation properties of resonators via temperature and optical signals offers potentially new avenues for applications in nano-scale heat regulation,²¹ detection,²² rectification,^{23,24} photovoltaics,²⁵ or incoherent sources.²⁶ We propose a practical, photonic structure where these effects can arise near room temperature and at mW powers.

The system under consideration belongs to the class of nonlinear photonic resonators depicted

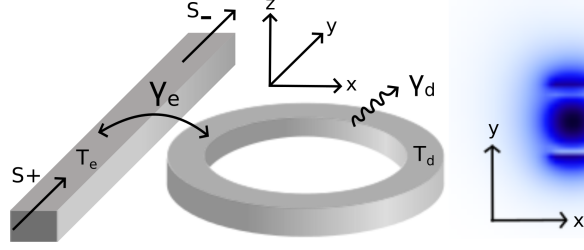


FIG. 1. Schematic of a wavelength-scale silicon ring resonator of radius $R = 4.4\mu\text{m}$, height $h = 220\text{nm}$, and width $w = 350\text{nm}$, coupled to a silicon waveguide (channel), both on a silica substrate. Also shown is the E_y mode profile of a resonance designed to have azimuthal number $m = 25$, wavelength $\lambda = 1.5\mu\text{m}$, radiative lifetimes $\gtrsim 10^6$, and relatively large nonlinear coupling coefficient $\alpha = 0.032\chi^{(3)}\omega_0/(8\epsilon_0\lambda^3)$. The loss γ_d and waveguide–coupling γ_e rates are much larger than the corresponding radiation rate.

in Fig. 1, involving a cavity coupled to an external channel (e.g. a waveguide). The description of thermal radiation in this system can be carried out via the coupled-mode theory framework²⁷, which we recently employed to study thermal radiation in a related system²⁸ but now extend to consider the addition of a coherent pump. The equations describing the cavity mode a are given by:²⁸

$$\frac{da}{dt} = [i(\omega_0 - \alpha|a|^2) - \gamma]a + \sqrt{2\gamma_d}\xi_d + \sqrt{2\gamma_e}s_+, \quad (1)$$

$$s_- = -s_+ + \sqrt{2\gamma_e}a, \quad (2)$$

where $|a|^2$ is the energy of the cavity mode and $|s_{\pm}|^2$ are the incident (+) and outgoing (–) power from and into the external channel, respectively. The latter arises due to dissipative noise inside the cavity ξ_d as well as externally incident light s_+ consisting of both thermal radiation ξ_e and a monochromatic pump $s_p \exp(i\omega_p t)$. The dynamics of the cavity field are described by its resonance frequency ω_0 and decay rate $\gamma = \gamma_e + \gamma_d$, which includes linear absorption γ_d as well as decay into the external channel γ_e . The real and imaginary parts of the nonlinear coefficient $\alpha = \frac{3}{4}\omega_0 \int \epsilon_0 \chi^{(3)} |\vec{E}|^4 / (\int \epsilon |\vec{E}|^2)^2$ depend on a complicated overlap integral of the linear cavity fields,²⁹ and lead to self-phase modulation (SPM) and two-photon absorption (TPA), respectively. We mainly focus on the effects of SPM (real $\alpha > 0$) since we find that TPA leads to thermal broadening of the kind explored in Ref. 28. Both internal and external thermal sources are represented by stochastic, delta-correlated white-noise sources ξ_e and ξ_d satisfying (assuming $\gamma \ll \omega_0$),

$$\langle \xi^*(t)\xi(t') \rangle = \Theta(\omega_0, T)\delta(t - t'), \quad (3)$$

where $\langle \dots \rangle$ denotes a thermodynamic or ensemble average, and $\Theta(\omega, T) = \hbar\omega / (e^{\hbar\omega/k_B T} - 1)$ is the mean energy of a Planck oscillator²³ at local temperature T ; the temperatures of the internal and external baths are denoted as T_d and T_e , respectively. Above, we assumed $\hbar\gamma/k_B \ll T_e, T_d$ allowing us to ignore the frequency-dispersion and temporal correlations (colored noise) associated with Θ . (Note that in the limit $\hbar\omega_0/k_B T \rightarrow 0$ one obtains the classical result $\Theta \rightarrow k_B T$.)

Thermal amplification and power tunability.— We show that bistability can amplify thermal fluctuations and lead to enhanced, temperature-tunable emission from the cavity. We begin by reviewing a number of key features of the system in the absence of thermal noise, whose contributions are considered perturbatively due to the generally weak nature of thermal noise, $|s_p|^2 \gg \gamma k_B T$. The steady-state cavity field a_0 due to the pump is given by the well-known cubic equation:^{13,30}

$$\left[\left(\Delta + \frac{\alpha|a_0|^2}{\gamma} \right)^2 + 1 \right] \frac{\alpha|a_0|^2}{\gamma} = 2\zeta, \quad (4)$$

where $\zeta \equiv \alpha|s_p|^2\gamma_e/\gamma^3$ is the effective nonlinear coupling associated with the pump and $\Delta \equiv \frac{\omega_p - \omega_0}{\gamma}$ is the dimensionless detuning. Equation (4) describes a number of extensively studied nonlinear effects,^{30,31} including bistability arising in the regime $\Delta < -\sqrt{3}$ and $\zeta^{(1)} < \zeta < \zeta^{(2)}$, as illustrated by the hysteresis plot on the inset of Fig. 2(a) which shows the dimensionless cavity energy $x = \alpha|a|^2/\gamma$ as a function of ζ .

An effect that seems little explored but that plays an important role on the thermal properties of this system is perfect absorption, which occurs when a photonic cavity is driven on resonance and its dissipation and radiation rates are equal, also known as rate matching.¹⁹ In the presence of nonlinearities, the cavity frequency and hence the absorbed power depend on ζ . For instance, in the non-bistable regime, the output power varies slowly with ζ , as illustrated by the green curve in Fig. 2(a) for $\Delta = -1$, increasing and then decreasing as $\zeta \rightarrow |\Delta/2|$, at which point the cavity and pump frequencies are in resonance, i.e. $\alpha|a_0|^2/\gamma = -\Delta$. Bistability can lead to a more pronounced dependence on ζ : the two stable steady states experience different frequency shifts and hence loss rates, and ultimately which state is excited in the steady state depends on the specific initial (or excitation) conditions.³² Figure 2(a) shows the steady-state output power $|s_-|^2$ as ζ is adiabatically increased (solid lines) from zero and above the critical point $\zeta^{(2)}$, for multiple Δ . The dashed blue line shows the power as ζ is adiabatically decreased below $\zeta^{(2)}$ for the particular case $\Delta = -2.5$, demonstrating that only the upper branch experiences perfect absorption, occurring at $\zeta = |\Delta/2|$

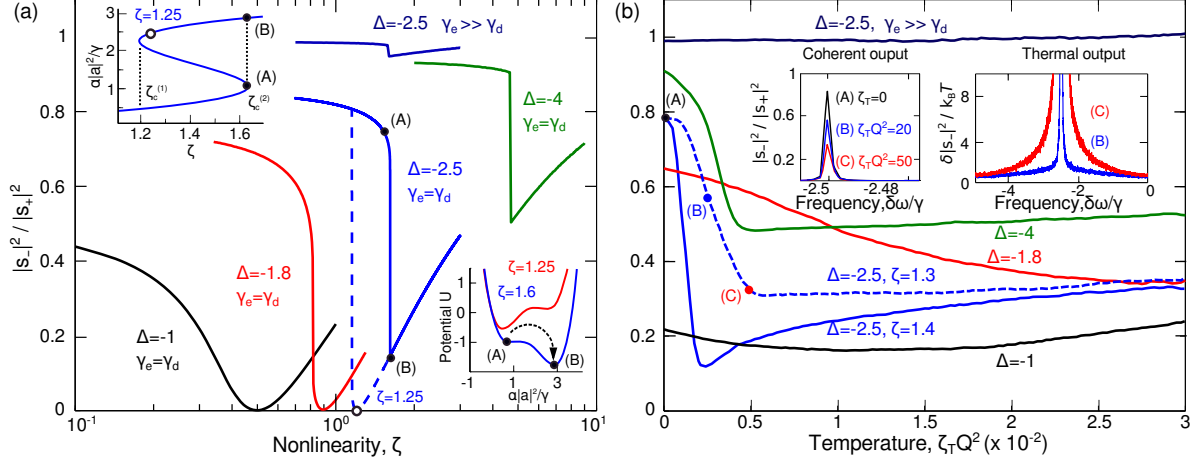


FIG. 2. (a) Output power $|s_-|^2$ normalized by the input power $|s_+|^2$ of the pumped system described in Fig. 1, in the absence of thermal noise and as a function of ζ , for different values of detuning $\Delta = \frac{\omega_p - \omega_0}{\gamma}$. The top left inset shows a hysteresis plot of the energy $\alpha|a_0|^2/\gamma$ as a function of ζ , the solutions of (4), for the particular choice of $\Delta = -2.5$ while the bottom inset shows the corresponding potential energy U as a function of the cavity energy for two different $\zeta = |\Delta/2|$ and $\zeta^{(2)}$. (b) The same normalized output power $|s_-|^2/|s_+|^2$ as a function of temperature $\zeta_T Q^2$, where $\zeta_T = \alpha\Theta(\omega_0, T)\gamma_e/\gamma^2$ and $Q = \omega_0/\gamma$, for different values of Δ and $\zeta \lesssim \zeta^{(2)}$. The insets illustrate the change in the coherent (left) and thermal radiation (right) spectra. Both internal and external baths have equal temperatures $T_d = T_e = T$.

and marked by the white circle. The corresponding change in the output power as the system transitions from the lower (A) to the higher (B) energy state at $\zeta^{(2)}$ is given approximately by:

$$|s_+|^2 \left(1 - \frac{\gamma_e - \gamma_d}{\gamma_e + \gamma_d} \right) \frac{(\Delta + x_1)^2 - (\Delta + x_2)^2}{[1 + (\Delta + x_1)^2][1 + (\Delta + x_2)^2]} \quad (5)$$

where $x_1 = -\frac{1}{3}(2\Delta + \sqrt{\Delta^2 - 3})$ and $x_2 = -2(\Delta + x_1)$ are the cavity energies associated with the lower and higher energy state, respectively. Given (5), one can show that the difference in output power is largest under the rate matching condition $\gamma_e = \gamma_d$ and at $\Delta \approx -7/3$, decreasing with smaller or larger detuning.

The presence of noise complicates this picture due to finite-temperature fluctuations which cause the system to undergo transitions between the two states, where the rates of forward/backward transitions are a complicated function of the potential energy U and temperature of the system.^{13,32} (For convenience and without loss of generality, we take both thermal baths to have the same temperature T .) In particular, U is obtained by integrating the steady-state equation associated with the cavity energy $\frac{dx}{dt} = [(\Delta + x)^2 + 1]x - 2\zeta = 0$ with respect to $x = \alpha|a|^2/\gamma$. Examples of U are shown on the lower inset of Fig. 2(a) for two values of ζ . Thermally activated hopping

leads to significant enhancement of amplitude fluctuations, which manifest as large changes in the radiation spectrum of the cavity. This is illustrated by the top inset of Fig. 2(b), which shows the thermal spectrum of the power $|\delta s_-(\omega)|^2$ for the particular choice of $\Delta = -2.5$ and $\zeta = 1.3$ and for multiple values of $\zeta_T Q^2$, where for convenience (below) we have introduced the dimensionless effective thermal coupling $\zeta_T \equiv \alpha \Theta(\omega_0, T) \gamma_e / \gamma^2$ and cavity-lifetime $Q = \omega_0 / \gamma$.¹⁹ Such enhancements were predicted to occur and recently observed in nonlinear mechanical oscillators,^{13,14} where the authors showed that at special ζ , the system undergoes a so-called kinetic phase transition associated with equal rates of forward/backward hopping and exhibits a “supernarrow” and highly amplified spectral peak. Interestingly, we find that in the case of optical resonators, thermal amplification can be accompanied by a significant decrease in the coherent output power despite the fact that $|s_p|^2 \gg \gamma k_B T$, a consequence of perfect absorption. In particular, operating under rate matching and near $\zeta^{(2)}$ allows for temperature to initiate transitions (A) \rightleftharpoons (B), leading to significant changes in $|s_-|^2$ with respect to T . Essentially, as $\zeta \rightarrow \zeta^{(2)}$, the potential barrier separating the lower x_1 from the higher x_2 energy states begins to disappear, resulting in increased rate of forward transitions and hence larger absorption.

These features are illustrated in Fig. 2(b) which shows the total output power as a function of $\zeta_T Q^2$ for different combinations of ζ and Δ . (We found numerically that for a given ζ and Δ , changing either ζ_T or Q^2 while leaving $\zeta_T Q^2$ unchanged leaves $|s_-|^2 / |s_+|^2$ unaltered.) Noticeably, while the change in the output power is gradual in the non-bistable regime ($\Delta > -\sqrt{3}$), there is a significantly stronger dependence in the bistable regime—the slope becomes increasingly sharper as $\zeta \rightarrow \zeta^{(2)}$ and $\zeta_T \rightarrow 0$ since it becomes increasingly easier for lower T fluctuations to induce hopping unto the higher-energy state. At sufficiently large ζ_T , $|s_-|^2$ is found to increase with increasing ζ_T as the cavity field no longer probes the hysteresis regime. While the maximum change in $|s_-|^2$ can be estimated from the steady-state analysis in the absence of noise (with the largest change occurring for $\Delta \approx -7/3$), its dependence on ζ_T is a complicated function of ζ and Δ . For instance, for $\Delta = -2.5$ and $\zeta = 1.4$ [blue line in Fig. 2(b)], the sharp decrease in output power occurs at $\zeta_T Q^2 \approx 10$ and yields a slope $\frac{1}{|s_+|^2} \frac{\delta(|s_-|^2)}{\delta(\zeta_T Q^2)} \approx 0.05$.

Side peaks.— We now show that the radiation spectrum also exhibits other interesting features, including the emergence of Raman-type Stokes and anti-Stokes side peaks previously observed in driven mechanical oscillators.^{13,14} Interestingly, we find that in our photonic resonator, the presence of the external channel dramatically alters the relative amplitudes of the side peaks, e.g. leading to a symmetric spectrum when the two baths have equal temperatures. We begin by ex-

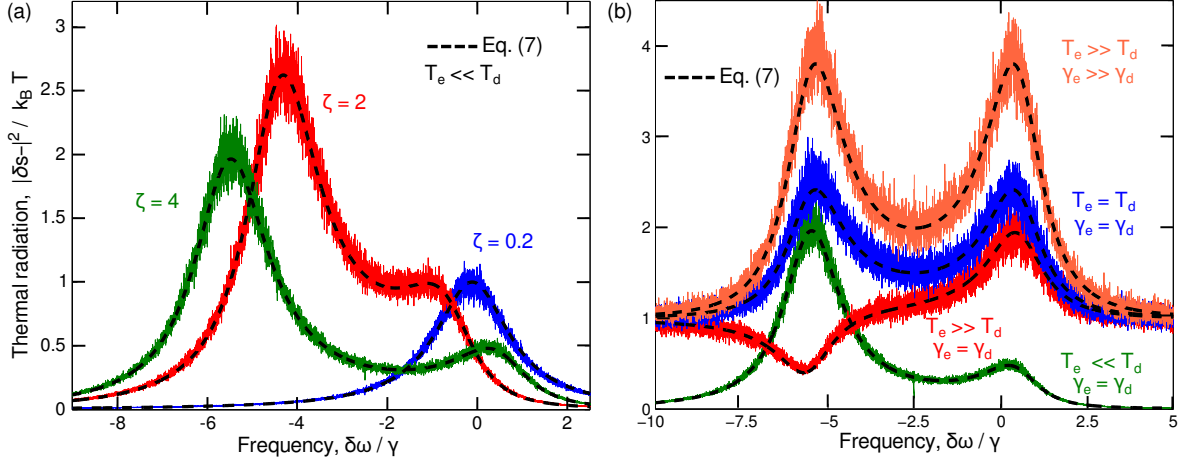


FIG. 3. Thermal radiation $|\delta s_-|^2$ for the system described in Fig. 1, normalized by the maximum of the internal and external bath temperatures $T = \max\{T_d, T_e\}$, as a function of the dimensionless frequency $\delta\omega/\gamma$ where $\delta\omega = (\omega - \omega_0)$, with fixed $\Delta = -2.5$ and under various operating conditions. The radiation spectrum is shown (a) in the limit $T_d \gg T_e$ of negligible externally incident radiation, for different values of ζ and (b) for fixed $\zeta = 4$ but different T_d, T_e and linear decay rates γ_d, γ_e .

exploiting a simple perturbation theory in which the thermal fluctuations of the cavity-field δa and radiation $\delta s_- = -\xi_e + \sqrt{2\gamma_e}\delta a$ are treated perturbatively, leading to analytical expressions for the corresponding thermal energy and radiation spectra. Assuming $|s_p|^2 \gg \gamma k_B\{T_d, T_e\}$, we obtain:

$$\langle |\delta a|^2 \rangle = \frac{k_B f_+ (2\gamma_d T_d + 2\gamma_e T_e)}{D} \quad (6)$$

$$\langle |\delta s_-|^2 \rangle = k_B T_e + \frac{4\gamma_e k_B}{D} [\gamma_d (f_+ T_d - f_- T_e) + \gamma_e (f_+ - f_-) T_e] \quad (7)$$

where f_+, f_- and D are given by

$$\begin{aligned} f_{\pm} &= (\omega + \omega_0 - 2\omega_p - 2\alpha|a_0|^2)^2 + \gamma^2 \pm \alpha^2|a_0|^4 \\ D &= [\gamma^2 + (\omega_0 - \omega_p - 2\alpha|a_0|^2)^2 - (\omega - \omega_p)^2 - \alpha^2|a_0|^4]^2 \\ &\quad + 4\gamma^2(\omega - \omega_p)^2, \end{aligned}$$

and where $|a_0|^2$ denotes the steady-state cavity energy in the absence of fluctuations, the solution of (4). Here, for simplicity we have assumed the classical limit $\Theta(\omega_0, T) \rightarrow k_B T$. In the absence of the external bath $T_e = 0$, the above equations are similar to those obtained in the case of mechanical oscillators.¹³ The situation changes with the channel due to the unavoidable interference and induced correlations of the emitted and reflected radiation, described in (7) by the f_- terms.

Figure 3 illustrates the radiation spectrum of the cavity under different operating conditions, showing excellent agreement between the numerically (noisy) and analytically (dashed lines) computed spectra. We note that all of the results shown in Fig. 3 correspond to cavities operating outside of the bistable regime: although it is possible to obtain a complete and analytical description of the spectrum based on (6) and (7), such an analysis is difficult in the bistable regime due to hopping between states, requiring a complicated description of the transition rates and stationary distributions of the system.¹³ For instance, in the bistable regime, one observes the appearance of a temperature-dependent supernarrow spectral peak whose amplitude decreases with increasing ζ . In the absence of bistability, a similar but weaker amplification occurs as $\zeta \rightarrow |\Delta/2|$ or equivalently, as the cavity frequency becomes resonant with the pump. Regardless of regime, at sufficiently large ζ (once the cavity resonance has crossed ω_p), modulation of the thermal noise by the pump causes the spectrum to transition from being singly to doubly resonant due to the emergence of an additional anti-Stokes peak.¹³ In the limit as $\zeta \rightarrow \infty$, both peaks move farther apart and their amplitudes asymptote to a system-dependent constant.

Figure 3(b) explores the dependence of the peak amplitudes on various cavity parameters, including $T_d = T_e$, $T_d \gg T_e$, and $T_d \ll T_e$, corresponding to a resonator that is either at thermal equilibrium, heated, or cooled with respect to its surroundings, respectively. When noise entering the system through the external bath is negligible $T_d \gg T_e$, similar to the previously explored situation involving mechanical oscillators,¹³ one finds that the Stokes peak is always much larger than the anti-Stokes peak (green line). Essentially, for $\alpha > 0$ the cavity nonlinearity favors down-conversion, as captured by the asymmetric f_+ terms above. The peak radiation associated with the Stokes peak can be readily obtained from (6) in the non-bistable regime $\Delta \leq -\sqrt{3}$, and is given by $\max |\delta s_-|^2 = \frac{4\gamma_e\gamma_d}{\gamma^2}(1 + 2\Delta^2)k_B T_d$, reaching $7k_B T_d$ precisely at the onset of bistability and when $\gamma_e = \gamma_d$. At larger $\zeta > |\Delta/2|$, the amplitude of both peaks decreases with increasing ζ where, as $\zeta \rightarrow \infty$ (not shown), the amplitude of the Stokes peak $\rightarrow k_B T_d$ while the anti-Stokes peak disappears. The situation changes dramatically when the noise entering the system through the external bath cannot be ignored, i.e. $T_e \gtrsim T_d$. In particular, as observed from (6), although the cavity spectrum favors Stokes to anti-Stokes conversion regardless of the relative temperatures or decay rates, we find that the spectrum of outgoing radiation can be dramatically different depending on the regime of operation. When $T_e \gg T_d$ where noise is dominated by external radiation, we find that the anti-Stokes peak dominates (red line) except when $\gamma_e \gg \gamma_d$, at which point the spectrum exhibits a symmetric lineshape (orange line). Such a reversal in relative am-

plitudes is captured by the f_- terms above, which include correlations and interference between the emitted and reflected radiation. The maximum radiation in the non-bistable regime in this case $\max |\delta s_-|^2 = k_B T_e (1 + \frac{8\gamma_e^2}{\gamma_d^2} \Delta^2 - \frac{4\gamma_e \gamma_d}{\gamma_d^2})$, reaching $25k_B T_e$ at the onset of bistability and when $\gamma_e \gg \gamma_d$ (rather than under rate matching). Interestingly, we find that when the two baths lie at the same temperature $T_e = T_d$, both peaks have equal amplitudes regardless of γ_e/γ_d , though the maximum amplitude in this regime also occurs in the limit $\gamma_e \gg \gamma_d$. This unexpected symmetrization of the spectrum arising due to interference effects seems to be a unique property of thermal radiation in this system. Although previous work on nonlinear fluctuations in the quantum regime observed similar peaks in the spectrum, a symmetric spectrum was found to arise only at zero temperature (a singular point of the theory³³) due to quantum tunneling.²⁰

Although a number of the abovementioned effects have been observed in mechanical oscillators, they remain unobserved in the context of thermal radiation where they could potentially be exploited in numerous applications.^{21,25,26} As demonstrated above, the interplay between the internal and externally incident radiation and the coherent pump leads to new effects in thermal radiators, including dramatic changes in both the coherent and thermal output spectrum with temperature, along with temperature-tunable Stokes and anti-Stokes side peaks. Finally, we conclude by proposing a realistic, silicon ring resonator design, depicted schematically in Fig. 1, where one could potentially observe these effects near room temperature and with operating $Q \sim 10^5$ and input power $|s_p|^2 \sim 1\text{mW}$, leading to $\alpha |s_p|^2 Q^2 \sim |\Delta|$. For these parameters we find that $\frac{1}{|s_+|^2} \frac{\delta(|s_-|^2)}{\delta(T)} \sim 0.04\text{K}^{-1}$ at $T \approx 300\text{K}$. Although this is almost two orders of magnitude smaller in comparison with thermo-optic effects in silicon, which lead to tunable powers $\sim \text{K}^{-1}$ for the same structure, at lower temperatures $T \lesssim 100\text{K}$ where the thermo-optic coefficient is much smaller³⁴, our fluctuation-induced effects offer significantly better temperature tunability. Other cavity designs such as the nanobeam cavity described in Ref. 35 yield much larger α and allow smaller Q to be employed, leading to even larger tunability compared to that obtained via thermo-optic effects.

We are grateful to Mark Dykman for very helpful comments and suggestions. This work was supported in part by the National Science Foundation under Grant No. DMR-145483.

REFERENCES

¹Kerry J. Vahala. Optical microcavities. *Nature*, 424:839–846, 2003.

²Tobias J. Kippenberg and Kerry J. Vahala. Cavity opto-mechanics. *Opt. Express*, 15(25):17172–

- 17205, 2007.
- ³R. Lifshitz and M.C. Cross. Nonlinear dynamics of nanomechanical and micromechanical resonators. *Reviews of nonlinear dynamics and complexity*, 1:1–50, 2008.
- ⁴Romain Quidant, Jan Gieseler, and Lukas Novotny. Thermal nonlinearities in a nanomechanical oscillator. *Nature Physics*, 9:806–810, 2013.
- ⁵J. Chaste, A. Eichler, J. Moser, G. Cellabos, R. Rurali, and A. Bachtold. A nanomechanical mass sensor with yoctogram resolution. *Nature Nanotechnology*, 7:301–304, 2012.
- ⁶A.N. Clelan and M.L. Roukes. Noise processes in nanomechanical resonators. *J. Appl. Phys.*, 92(5):2758–2769, 2002.
- ⁷R. Almog, S. Zaitsev, O. Shtempluck, and E. Buks. High intermodulation gain in a micromechanical duffing resonator. *Appl. Phys. Lett.*, 88:213509, 2006.
- ⁸Mark Dykman, editor. *Fluctuating Nonlinear Oscillators: From Nanomechanics to Quantum Superconducting Circuits*, chapter 13. Oxford University Press, 2012.
- ⁹Ling-An Wu, Min Xiao, and H. J. Kimble. Squeezed states of light from an optical parametric oscillator. *JOSA-B*, 4:1465–1476, 1987.
- ¹⁰Luca Gammaltoni, Peter Hangi, Peter Jung, and Fabio Marchesoni. Stochastic resonance. *Rev.Mod.Phys.*, 70:223, 1998.
- ¹¹M.I. Dykman. Theory of nonlinear nonequilibrium oscillators interacting with a medium. *Zh.Eksp.Theor.Fiz*, 68:2082–2094, 1975.
- ¹²M.I. Dykman and P.V.E. McClintok. Power spectra of noise-driven nonlinear systems and stochastic resonance. *Physica D*, 58:10–30, 1992.
- ¹³M.I. Dykman, D.G. Luchinsky, and R. Manella. Supernarrow spectral peaks and high-frequency stochastic resonance in systems with coexisting periodic attractors. *Physical Review E*, 49(2):1198–1215, 1994.
- ¹⁴C. Stambaugh and H.B. Chan. Supernarrow spectral peaks near a kinetic phase transition in a driven nonlinear micromechanical oscillator. *Phys. Rev. Lett.*, 97:110602, 2006.
- ¹⁵C. Stambaugh and H.B. Chan. Noise-activated switching in a driven nonlinear micromechanical oscillator. *Phys. Rev. B*, 73:172302, 2006.
- ¹⁶Stephan Andre, Lingzhen Guo, Vittorio Peano, Michael Mathaler, and Gerd Schon. Emission spectrum of the driven nonlinear oscillator. *Phys. Rev. A*, 85:053825, 2012.
- ¹⁷Masaya Notomi, Akihiko Shinya, Satoshi Mitsugi, Goh Kira, Eiichi Kuramochi, and Takasumi Tanabe. Optical bistable switching action of Si high- q photonic-crystal nanocavities. *Opt. Ex-*

- press*, 13(7):2678–2687, 2005.
- ¹⁸A. R. Cowan and J. F. Young. Optical bistability involving photonic crystal microcavities and fano line shapes. *Phys. Rev. E*, 68:046606, 2003.
- ¹⁹John D. Joannopoulos, Steven G. Johnson, Joshua N. Winn, and Robert D. Meade. *Photonic Crystals: Molding the Flow of Light*. Princeton University Press, second edition, February 2008.
- ²⁰P.D. Drummond and D.F. Walls. Quantum theory of optical bistability *I*. nonlinear polarisability model. *Journal of Physics A: Math. and Gen.*, 13:725, 1980.
- ²¹Lei Wang and Baowen Li. Thermal memory: A stroage of phononic information. *Phys. Rev. Lett.*, 101:267203, 2008.
- ²²Kengo Nozaki, Shinji Matsuo, Koji Takeda, Tomonari Sato, Eiichi Kuramochi, and Masaya Notomi. Ingaas nano-photodetectors based on photonic crystal waveguide including ultracompact burried heterostructure. *Optics Express*, 21:19022, 2013.
- ²³Clayton R. Otey, Wah Tung Lau, and Shanhui Fan. Thermal rectification through vacuum. *Phys. Rev. Lett.*, 104(15):154301, 2010.
- ²⁴Nick A. Roberts and D.G. Walker. A review of thermal rectification observations and models in solid materials. *Journal of Thermal Sciences*, 50:648–662, 2011.
- ²⁵Andrej Lenert, David M. Bierman, Youngsuk Nam, Walker R. Chan, Ivan Celanovic, Marin Soljacic, and Evelyn N. Wang. A nanophotonic solar thermophotovoltaic device. *Nature Nanotechnology*, 9:126–130, 2014.
- ²⁶S. Noda, M. Fujita, and T. Asano. Spontaneous-emission control by photonic crystals and nanocavities. *Nature Photonics*, 1:449–458, 2007.
- ²⁷H. A. Haus. *Waves and Fields in Optoelectronics*. Prentice-Hall, Englewood Cliffs, NJ, 1984. Ch. 7.
- ²⁸Chinmay Khandekar, Adi Pick, Steven G. Johnson, and Alejandro W. Rodriguez. Radiative heat transfer in nonlinear kerr media. *Phys. Rev. B*, 91:115406, 2015.
- ²⁹Alejandro Rodriguez, Marin Soljačić, J. D. Joannopulos, and Steven G. Johnson. $\chi^{(2)}$ and $\chi^{(3)}$ harmonic generation at a critical power in inhomogeneous doubly resonant cavities. *Opt. Express*, 15(12):7303–7318, 2007.
- ³⁰Marin Soljacic, Mihai Ibanescu, Steven J. Johnson, Yoel Fink, and J.D. Joannopoulos. Optimal bistable switching in nonlinear photonic crystals. *Phys.Rev.E.*, 66:055601, 2002.
- ³¹Steven G. Johnson, Attila Mekis, Shanhui Fan, and J. D. Joannopoulos. Molding the flow of

light. *Computing Sci. Eng.*, 3(6):38–47, 2001.

³²Steven H. Strogatz. *Nonlinear Dynamics and Chaos*. Westview Press, Boulder, CO, 1994.

³³M.I. Dykman and M.A. Krivoglaz. Theory of nonlinear oscillators interacting with a medium. *Soviet Physics Reviews*, 5, 1984.

³⁴J. Komma, C. Schwarz, G. Hoffman, D. Heinert, and R. Nawrodt. Thermo-optic coefficient of silicon at 1550nm and cryogenic temperatures. *Appl. Phys. Lett.*, 101:041905, 2012.

³⁵Z. Lin, T. Alcorn, M. Loncar, S.G. Johnson, and A.W. Rodriguez. High-efficiency degenerate four wave-mixing in triply resonant nanobeam cavities. *Phys. Rev. A*, 89:053839, 2014.